

**ICSO 2016**

**International Conference on Space Optics**

Biarritz, France

18–21 October 2016

*Edited by Bruno Cugny, Nikos Karafolas and Zoran Sodnik*



***AOTF spectrometers in space missions and their imaging capabilities***

*Oleg Korablev*

*Alexander Y. Trokhimovsky*

*Yurii K. Kalinnikov*



icso proceedings



## AOTF SPECTROMETERS IN SPACE MISSIONS AND THEIR IMAGING CAPABILITIES

O. I. Korablev<sup>1</sup>, A. Yu. Trokhimovskiy<sup>1</sup>, Yu. K. Kalinnikov<sup>2</sup>

<sup>1</sup>*Space Research Institute (IKI), Russia.* <sup>2</sup>*National Research Institute for Physical-technical and Radiotechnical Measurements (VNIIFTRI), Russia.*

### I. INTRODUCTION

Acoustooptic tunable filter (AOTF) is an electronically tunable optical filter, using the principle of Bragg's diffraction of an entrance beam on the ultrasonic acoustic wave excited within a birefringent crystal. A variable radio frequency (RF) signal, typically below few watts, is applied to a piezoelectric transducer bonded to the crystal. The filter can be then randomly tuned to any desired wavelength within its spectral range. So-called wide-aperture AOTFs, the most applicable for spectrometry were demonstrated in the 1970-ies [1, 2]. The AOTF filters are technologically mature (a similar technology has been well developed for mass production of beam deflectors), and compact AOTF-based spectrometers and cameras are widely used for astronomy, process control, medicine, research, etc. mostly in the near-IR and visible spectral ranges [3-7].

There is no moving part in an AOTF spectrometer, not counting a solid-state ultrasound actuator, so it can be built as a relatively simple, low mass, rugged, and durable device. The mostly used filter material, the paratellurite TeO<sub>2</sub> is suitable for a wide range of 0.4-5  $\mu\text{m}$  and is immune to radiation. These qualities suggest their high potential in space-borne devices, and numerous developments towards the use of the AOTF technology in space were conducted. However, few devices have finally reached space. They were used as such, and for separation of orders in high-resolution échelle spectrometers. The imaging capability of AOTFs is often discussed as an important advantage, e.g. [8], however for remote (not close-up) sensing the imaging has not been really implemented yet.

In the present paper we briefly review the space-borne AOTF spectrometers reported in the open literature, discuss advantages, limitations and perspectives of their implementation in space, with an emphasis on imaging capabilities of an AOTF and the échelle-AOTF combination.

### II. THE AOTFS IN SPACE

The AOTF spectrometers flown in space published in an open literature are summarized in Table 1. Many of them are pencil-beam devices, or are derivatives of the same functionality. The first – to our knowledge – instrument was flown in 1986 on the first satellite of the Okean NHM (Ocean –for general purpose) series (also designated as Kosmos-1766). It operated in the visible range with two PMT detectors for two orthogonal polarisations. Data collected from near-polar  $\sim 650$  km orbit during about one year of operation were used in marine research [9]. A very similar instrument was later flown on a new generation Okean-O satellite.

For an interplanetary mission the requirement of the low mass and volume often becomes a decisive factor. For the Mars Express mission by ESA SPICAM (Spectroscopy for the Investigation of the Characteristics of the Atmosphere of Mars) was out of the model payload of the Mars Express project. Only an extremely lightweight near-IR spectrometer for the range of 0.9–1.7  $\mu\text{m}$  based on AOTF technology was accepted by ESA as the IR channel of SPICAM [10-12]. The Mars Express orbiter has started science operations in January 2004. Since then its suite of optical instruments is observing Mars from a  $300 \times 10,100$  km elliptical orbit, mostly in the pericenter (nadir viewing), but also on the limb, and using solar occultation technique. The infrared channel of SPICAM, the first example of an AOTF in deep space remains fully operational after 12 years in the Mars orbit and delivers information about the planetary water cycle and the atmosphere. The next planetary mission by ESA, Venus Express orbited Venus in April 2006. The 24-h polar elliptical orbit ranged between 66,000 and 250 km above the surface with pericenter close to the North Pole (80°N). At this time the mission science payload has included already two AOTF devices. Spectroscopy for the Investigation of the Characteristics of the Atmosphere of Venus/ Solar Occultation in the InfraRed (SPICAV/SOIR) instrument [13] consists of three independent spectrometers, including an ultraviolet grating spectrometer with an intensified CCD (118–320 nm), near infrared acousto-optic (650–1700 nm, spectral resolution better than 1 nm) SPICAV IR, and infrared échelle-spectrometer with acousto-optic selection of diffraction orders SOIR for the spectral range of 2.2–4.3  $\mu\text{m}$  (resolving power  $\sim 20,000$ ). While the SPICAV IR is basically a derivative from SPICAM IR channel on Mars Express, a pencil-beam AOTF spectrometer modified to adapt for Venus nightside observations [14], SOIR represents the first space implementation of a new spectrometer type.

The principle of the acousto-optic selection of diffraction or interferential orders is obvious. When the number of orders is large, like in Fabry-Perot interferometer, Michelson echelon, or the échelle-spectrometer, the random access and the fine tuning of an AOTF allows to pick any of the desired orders for further analysis, achieving the desired high spectral resolution in a relatively simple scheme (Fig. 1). The bandwidth of the AOTF can be matched to the free spectral range of the échelle spectrometer to achieve a nearly continuous spectral coverage. Comparing to, e.g., cross-dispersion scheme this implementation of order-sorting allows for much reduced volume, and therefore the overall mass and complexity of the instrument. The combination échelle-AOTF has been first demonstrated for an analytical application [15], and soon proposed as a perspective tool in atmospheric and planetary space studies [16, 17]. SOIR built in Belgium for Venus Express [18] has become the first space instrument of that type. SOIR, operating since 2006 exclusively in solar occultations allowed to obtain vertical profiles of minor constituents in the Venusian atmosphere, and important isotope ratios. In the following, a pilot experiment RUSALKA (Russian acronym for handheld Spectral AnaLYser for Constituents of Atmosphere, also stands for the mermaid) to demonstrate the possibility to measure the greenhouse gases in the terrestrial atmosphere using a SOIR-type instrument in the spectral range 0.7-1.7  $\mu\text{m}$  was realized on ISS [19]. Different cosmonaut crews operated RUSALKA from 2009 through 2012. The atmosphere was observed from the pressurized compartment of ISS through illuminators. Also, a simplified version of SOIR aimed to study the minor constituents of the Martian atmosphere was developed and launched on board unsuccessful Phobos Grunt Russian mission (2011) [20]. Recently three échelle-AOTF instruments have been launched onboard ExoMars Trace Gas Orbiter. Two main channels of NOMAD (Nadir and Occultation for Mars Discovery) instrument are close derivatives of SOIR/Venus Express [21]. The near-IR channel of Atmospheric Chemistry Suite (ACS) is an improved version of RUSALKA [22]. These instruments were already operated in space.

For the future, the ALTUIS (Atmospheric Limb Tracker for the Investigation of the Upcoming Stratosphere) instrument is in development for studies of the terrestrial atmosphere. This Belgian project is intended for a microsatellite to study the ozone and other constituents profile at the limb using imaging AOTF channels in the visible and near IR ranges [23, 24].

Many spectrometers were and are being developed for mineralogy analysis at the surface of other planets. AOTF-based spectrometers for aerospace applications were developed in JPL [25], in France during the early phase of the project which has then became Rosetta, in GSFC [26, 27]. AOTFs are generally prone to temperature below  $-80^{\circ}\text{C}$ , and the temperature operation/storage range may be critical in the harsh environment on the surface of another planet [28]. Because of that a microscope-spectrometer ÇIVA for Rosetta mission has been finally developed using a traditional grating monochromator. Some progress was achieved during preparation of a microscope-spectrometer with monochromatic illumination of a sample using the AOTF for Phobos Grunt mission [29, 30]. A similar MicrOmega instrument is en route to asteroid launched in December 2014 on board Hayabusa-2 JAXA mission [31]. It is also a part of the analytical laboratory of the ExoMars 2020 rover mission [32]. AOTF spectrometers for surface characterization were developed in China; one of them successfully flown on Chang'e-3 lunar mission [33, 34]. Similar pencil-beam AOTF spectrometers are being developed for Russian lunar landers, and to be installed at the ExoMars 2020 rover mast [35]. Finally, an AOTF point spectrometer is being developed as a channel of SuperCam instrument for NASA Mars 2020 Rover [36].

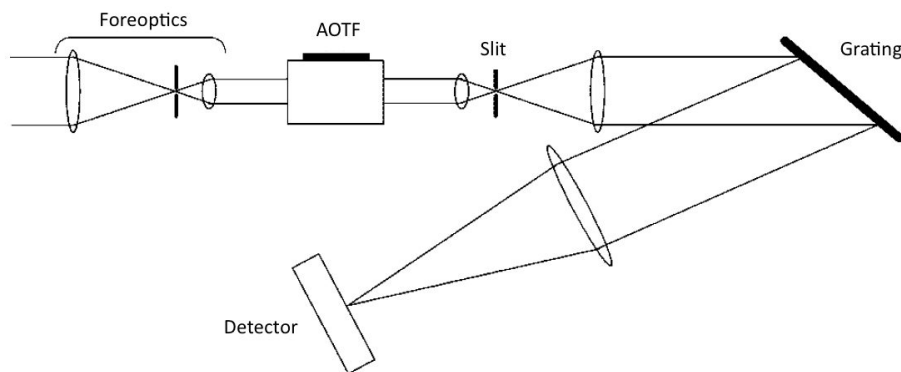


Fig. 1. A simplified optical scheme of échelle-AOTF spectrometer (adopted from [18])

Concluding, most of the AOTF spectrometers flown in space (see Table 1) are pencil-beam devices, or are derivatives of the same functionality.

Table 1. AOTF devices flown and operated in space.

Year(s)	Spacecraft	Instrument name, target	Filter material, Spectral range	Principle, observation	References
1986	Okean-NHM, USSR	Trasser Ocean colour	Quartz 0.42-0.78 $\mu\text{m}$	Pencil-beam, nadir	[9, 37]
1999	Okean-O, Russia	-“-	Quartz 0.41-0.81 $\mu\text{m}$	-“-	[37]
2003-pres.	Mars Express, ESA	SPICAM-IR Mars atmosphere	TeO <sub>2</sub> 0.9-1.65 $\mu\text{m}$	Pencil-beam, nadir, limb, solar occultation	[12, 38]
2005-2014	Venus Express, ESA	SPICAV-IR Venus atmosphere	TeO <sub>2</sub> 0.65-1.6 $\mu\text{m}$	Pencil-beam, nadir, limb, solar occultation	[14]
-“-	-“-	SOIR Venus atmosphere	TeO <sub>2</sub> 2.2-4.4 $\mu\text{m}$	Order-sorting in échelle-spectrometer solar occultation	[18]
2009-2012	ISS, Russian segment	RUSALKA greenhouse gases	TeO <sub>2</sub> 0.7-1.7 $\mu\text{m}$	Order-sorting in échelle-spectrometer Nadir	[19]
2013	Chang’e-3 Yutu, CNSA	VNIS Moon mineralogy	0.45–0.95 $\mu\text{m}$ 0.9–2.4 $\mu\text{m}$ TeO <sub>2</sub>	Imaging Pencil-beam both in reflection	[34]
2014 in flight	Hayabusa-2 MASCOT, JAXA, DLR/CNES	MicrOmega Mineralogy of asteroid	0.9-3.55 $\mu\text{m}$ TeO <sub>2</sub>	Monochromatic illumination of a sample	[31]
2016 in flight	ExoMars TGO, ESA/Roscosmos	ACS-NIR NOMAD-LNO NOMAD-SO Mars atmosphere	0.7–1.65 $\mu\text{m}$ 2.3–3.8 $\mu\text{m}$ 2.2-4.2 $\mu\text{m}$ TeO <sub>2</sub>	Nadir, limb, SO Nadir, SO SO Order-sorting in échelle-spectrometer	[21, 22]

### III. IMAGING AOTFS

Even if not designated as “imaging,” any wide-aperture AOTF conserves the image and in some designs mentioned above is used to form a field of view, or, with an imaging detector, to resolve 1-D or 2-D patterns. As discussed above the idea of using AOTF spectrometer for remote sensing from orbit is very attractive. It was advocated in the literature and a number a prototypes is developed, however, with few exceptions, the AOTF-based imaging spectrometers have not been flown so far. There are three basic reasons for that.

Let us consider a reference push-broom spectrometer recording a swath of  $n$  elements and resolving, for simplicity,  $n$  spectral bins, and compare it to a frame  $n \times n$  AOTF spectrometer, also with  $n$  spectral bins. The considerations below could be easily generalized for different raster and spectral dimensions. Let us assume also that the exposure time  $t$  matches to the smear so that the surface resolution along the spacecraft velocity is the same as in perpendicular direction. At each moment the push-broom device records a stripe perpendicular to the velocity vector, and each point corresponds to a spectrum, giving in all  $n^2$  counts. The next exposure forms the second line of the spectro-image, etc. In turn the AOTF device records a frame ( $n^2$ ), followed by a shifted frame in the next spectral bin, and so on. When the spacecraft moves continuously along the orbit the two spectrometers collect equivalent amount of information per second. However, with the AOTF sequential spectral record each spectral bin corresponds to different footprint, and the conventional data analysis pipeline should be seriously rearranged, and becomes non-trivial if some conditions, the phase angle for instance, is changing. Furthermore, the frame acquisition results in edge effects: The first and the last  $n$  frames of an orbit are incomplete. In a real observation, with clouds, each interruption or transition costs  $n^3$  to  $2n^3$  in data volume and  $nt$  to  $2nt$  in observation time, and is not negligible.

The second problem is related to spatial resolution of the AOTF. It is diffraction-limited and determined by the size of a crystal and its acceptance angle. In practical terms it is limited to 500, at most 1000 lines that is far below the modern requirements on swath/ground resolution.

The third and the most important problem is the sensitivity of the AOTF instruments. The effectiveness of an AOTF, typically 60-80% in maximum, is well compatible with that of a grating. However the AOTF conserves only one polarization, therefore the loss is twofold. A number of hints to recover and recombine the both polarizations is reported, e.g., [39], but none seems compatible with a real remote sensing imager. Also, because of the crystal size/acceptance angle limitation, the AOTF spectrometers have limited étendue, generally below  $f:3.5$ - $f:4$ . Compared to grating or prism devices, which could be as open as  $f:1$ - $f:1.5$  or even better, they therefore suffer a factor of  $\sim 10$  in quantum efficiency. To compensate for the overall factor of  $\sim 20$  by an increase of exposure time is unrealistic and this latter problem becomes prohibitive for applications where the quantum efficiency is essential.

The above factors make the traditional “push-broom” design preferable for a spectral imaging from the orbit. The imaging AOTF remains suitable for more specific niches when the mass and complexity issues are decisive. One obvious application is observation of a static or slow moving scene, e.g., from a synchronized orbit, planetary lander or rover. Indeed the only imaging AOTF flown to date is the visible channel of the Chinese VNIS instrument operated on Yutu rover [34]. In this case the frame imaging becomes an advantage (no scanning needed), and the depleted sensitivity could be compensated by longer exposure time. Another possibility is to make use of the AOTF random tuning and to observe the scene using only selected wavelengths of interest. More specific cases of observation geometry are possible, like with the ALTIUS imagers observing the atmosphere at the limb in a limited angular range. Below we consider the case of imaging using the echelle-AOTF spectrometer.

#### IV. AN IMAGING ECHELLE-AOTF SPECTROMETER

The near-Infrared echelle-AOTF spectrometer is one channel of the Atmospheric Chemistry Suite (ACS) package dedicated for the studies of the Martian atmosphere on board ExoMars Trace Gas Orbiter launched in 2016 [20]. The near-infrared (NIR) channel of ACS is a versatile spectrometer for the spectral range of 0.7–1.6  $\mu\text{m}$  with a resolving power of  $>20,000$ . A simplified optical scheme of the NIR channel is presented in Fig. 2. To enhance the sensitivity for lower signal nadir observations we use a high slit in combination with  $640 \times 512$  array detector allowing to capture the flux of the dispersed light along the full dimension of the slit. Although imaging capabilities along the slit initially were not considered for ACS NIR, its design may be suggested as groundwork for the imaging AOTF-echelle spectrometers.

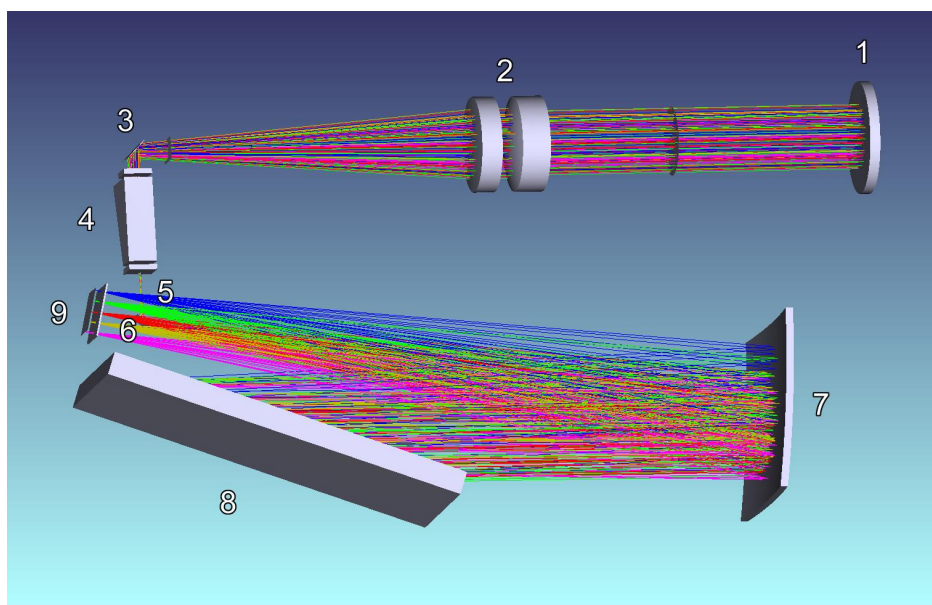


Fig. 2. A simplified optical scheme of the ACS NIR. 1- blocking longpass filter; 2- entry telescope; 3, 6- folding mirrors, 4- AOTF crystal, 5- slit, 7- main collimating mirror of the spectrometer, 8- diffraction grating, 9- detector array.

The custom-developed AOTF is operating in the 0.7–1.6  $\mu\text{m}$  spectral range with  $70\text{ cm}^{-1}$  spectral response function and F/6 aperture (9.6 degrees). In contrast to previously implemented design solutions, the acousto-optic filter is placed in a converging beam and close to the slit. The central light beam is propagating at an angle of  $36^\circ$  to the main optical axis [001] of the acousto-optic crystal  $\text{TeO}_2$ . This large angle allows to increase the AOTF aperture, while requiring to use higher RF range. With the slit being close to the AOTF the linear aperture of the filter is oblong and composes approximately  $2 \times 6\text{ mm}$ . That allowed to narrow the acoustic field inside the crystal and to implement the piezoelectric transducer of only 2 mm wide. This in turn allows for reducing the RF power: the light diffraction efficiency reaches 70% already with 2 Watts of the overall AOTF consumption.

The foreoptics (2 in Fig. 2) is designed with respect to the dispersion properties of the AOTF crystal. Two entry doublets (not distinguishable in Fig. 2) ensure high transparency of the system and uniform slit illumination. The entrance telescope has a focal length of 120 mm and the  $4\text{ mm} \times 40\text{ }\mu\text{m}$  slit is forming the instrument FOV of approximately  $2^\circ \times 0.02^\circ$  ( $35 \times 0.35\text{ mrad}$ ). The foreoptics and the AOTF conserve the image of the observed scene on the slit with good spatial resolution. Energy concentration within  $20 \times 20\text{ }\mu\text{m}^2$  pitch is above 0.85.

The echelle-spectrometer employs the Littrow auto-collimation scheme, in which an off-axis parabolic mirror plays the role of the collimating and the imaging elements. Spectral resolution is limited by the slit width and aberrations of the off-axis parabolic collimator. The spectral resolving power is defined by the spread function width and variable over the detector [20], but remains always  $\geq 20,000$ . The spread function width changes very slightly along the slit, and this determines almost constant spatial resolution for each wavelength. The pixel pitch is  $20 \times 20\text{ }\mu\text{m}^2$  and in the central part of the detector, where AOTF spectral response function is in maximum, the image is conserved with a resolution better than 1 pixel. Although to the edges of the detector aberrations worsen both, the picture and the spectra. Within a diffraction order the quality of the image degrades up to a factor of two towards the edges of the detector (Fig. 3).

The spatial resolution of the instrument was tested during adjustments and tests of the ACS NIR flight model. A millimeter-scale illuminated pattern was imaged from the distance of 5 meters. An element of 1 mm projected through the AOTF onto the spectrometer's slit then forms a 1-pixel image in the center of the detector. From the ExoMars-2016 TGO 400-km circular orbit an instantaneous ground resolution in nadir will be 80 meters, and at the limb in occultation – about 300 meters. This gives an opportunity to use the spatial resolution for observing local atmospheric phenomena.

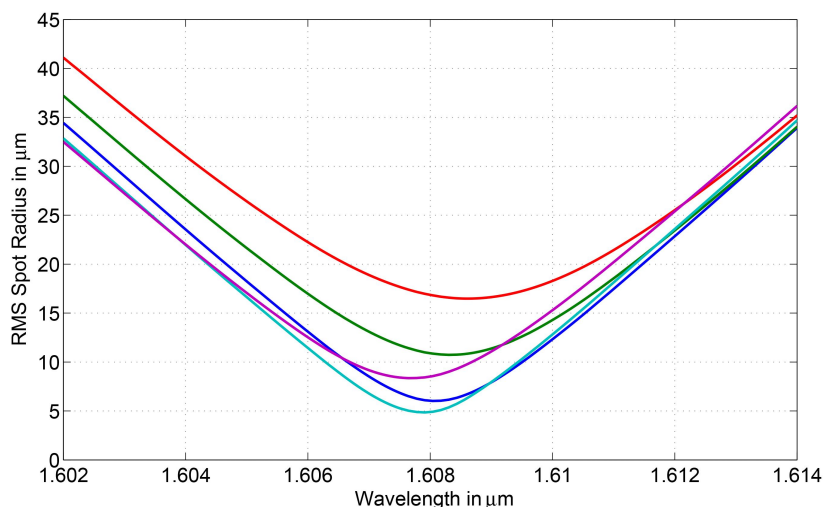


Fig. 3. RMS spot radius within one diffraction order of the AOTF-echelle spectrometer. The wavelength (x-axis) spans across the full width of the detector. Different colors stand for different positions along the slit (the spatial resolution).

## V. COLCLUSIONS

Spectrometers employing acousto-optic tuneable filters (AOTFs) rapidly gain popularity in space, and in particular on interplanetary missions. They allow for reducing volume, mass and complexity of the instrumentation. There are however serious issues with implementing imaging AOTFs for remote sensing. They are related to sequential spectral scanning, and to limited étendue of the acousto-optic devices. Nevertheless the imaging capabilities of the filters can be successfully realized in specific applications, such as analysis of static and brightly illuminated scenes, as well as in specific narrow-angle applications. The imaging capabilities of one of such applications, the échelle-AOTF spectrometer are discussed. The current design allows to resolve up to 200 elements within the 2° FOV (along the slit). This feature can be used for planning future applications for spectrometers with similar design.

## REFERENCES

- [1] I. C. Chang, "Noncollinear acoustooptic filter with large angular aperture," *Appl. Phys. Lett.* **25**, 370-372 (1974).
- [2] T. Yano, and A. Watanabe, "New acousto-optic tunable filter using far off axis diffraction in TeO<sub>2</sub>," *IEEE J. Quant. Electronics* **10**, 758-759 (1974).
- [3] H. Li, Y. Zhang, C. Wen, and Y. C. Soh, "Design of Tunable Composite Spectrums Using All-Fiber Acoustooptical Filters Subject to Strain Control," *J. Lightwave Technol.* **24**, 1855 (2006).
- [4] Q. Li, D. Xu, X. He, Y. Wang, Z. Chen, H. Liu, Q. Xu, and F. Guo, "AOTF based molecular hyperspectral imaging system and its applications on nerve morphometry," *Applied Optics* **52**, 3891-3901 (2013).
- [5] Y. Yuan, J.-Y. Hwang, M. Krishnamoorthy, K. Ye, Y. Zhang, J. Ning, R. C. Wang, M. J. Deen, and Q. Fang, "High-throughput acousto-optic-tunable-filter-based time-resolved fluorescence spectrometer for optical biopsy," *Opt. Lett.* **34**, 1132-1134 (2009).
- [6] N. J. Chanover, D. G. Voelz, D. A. Glenar, and E. F. Young, "AOTF-Based Spectral Imaging for Balloon-Borne Platforms," *J. Astron. Instrum.* **3**, 1440005 (2014).
- [7] V. Y. Molchanov, S. P. Anikin, S. I. Chizhikov, K. B. Yushkov, O. Y. Makarov, A. M. Tatarnikov, S. A. Potanin, and V. F. Esipov, "Acousto-optical imaging spectropolarimetric devices: new opportunities and developments," *Proc. SPIE* **9147**, 91472T (2014).
- [8] H. Kurosaki, "Earth observation by the adaptive wavelength optical image sensor," *Adv. Space Res.* **39**, 185-189 (2007).
- [9] S. N. Korolev, A. A. Kucheryavii, V. A. Mironenko, and V. S. Suetin, "Use of the Trasser apparatus to observe the ocean from space," *Soviet J. of Remote Sens.* **10**, 620-631 (1993).
- [10] J. Bertaux, D. Fonteyn, O. Korablev, E. Chassefiere, E. Dimarellis, J. Dubois, et al., "The study of the Martian atmosphere from top to bottom with SPICAM light on Mars Express," *Planet. Space Sci.* **48**, 1303-1320 (2000).
- [11] O. Korablev, J.-L. Bertaux, A. Grigoriev, E. Dimarellis, Y. Kalinnikov, A. Rodin, et al., "An AOTF-based spectrometer for the studies of Mars atmosphere for Mars Express ESA mission," *Adv. Space Res.* **29**, 143-150 (2002).
- [12] O. Korablev, J. Bertaux, A. Fedorova, D. Fonteyn, A. Stepanov, Y. Kalinnikov, et al., "SPICAM IR acousto-optic spectrometer experiment on Mars Express," *J. Geophys. Res.* **111**, E09S03- (2006).
- [13] J. Bertaux, D. Nevejans, O. Korablev, E. Villard, E. Quemerais, E. Neefs, et al., "SPICAV on Venus Express: Three spectrometers to study the global structure and composition of the Venus atmosphere," *Planet. Space Sci.* **55**, 1673-1700 (2007).
- [14] O. Korablev, A. Fedorova, J.-L. Bertaux, A. V. Stepanov, A. Kiselev, Y. K. Kalinnikov, et al., "SPICAV IR acousto-optic spectrometer experiment on Venus Express," *Planet. Space Sci.* **65**, 38-57 (2012).
- [15] D. P. Baldwin, D. S. Zamzow, D. E. Eckels, and G. P. Miller, "AOTF-echelle spectrometer for air-ICP-AES continuous emission monitoring of heavy metals and actinides," *Proc. SPIE* **3853**, 213 (1999).
- [16] O. I. Korablev, J.-L. Bertaux, and I. I. Vinogradov, "Compact high-resolution IR spectrometer for atmospheric studies," *Proc SPIE* **4818**, 272 (2002).
- [17] O. I. Korablev, J.-L. Bertaux, I. I. Vinogradov, Y. K. Kalinnikov, D. Nevejans, E. Neefs, et al., "Compact high-resolution echelle-AOTF NIR spectrometer for atmospheric measurements," in *Proceedings of the 5th International Conference on Space Optics (ICSO 2004)*, ESA SP **554**, 73-80 (2004).
- [18] D. Nevejans, E. Neefs, E. Van Ransbeeck, S. Berkenbosch, R. Clairquin, L. De Vos, et al., "Compact high-resolution spaceborne echelle grating spectrometer with acousto-optical tunable filter based order sorting for the infrared domain from 2.2 to 4.3 μm," *Appl. Opt.* **45**, 5191-5206 (2006).
- [19] O. Korablev, A. Trokhimovskii, I. Vinogradov, A. Fedorova, A. Ivanov, A. Venkstern, et al., "The RUSALKA device for measuring the carbon dioxide and methane concentration in the atmosphere from on board the International Space Station," *J. Optical Technol.* **78**, 317-327 (2011).

- [20] O. Korablev, F. Montmessin, A. Trokhimovsky, A. A. Fedorova, A. V. Kiselev, J.-L. Bertaux, et al., "Compact echelle spectrometer for occultation sounding of the Martian atmosphere: design and performance," *Appl. Opt.* **52**, 1054-1065 (2013).
- [21] E. Neefs, A. C. Vandaele, R. Drummond, I. R. Thomas, S. Berkenbosch, R. Clairquin, et al., "NOMAD spectrometer on the ExoMars trace gas orbiter mission: part 1—design, manufacturing and testing of the infrared channels," *Appl. Opt.* **54**, 8494 (2015).
- [22] A. Trokhimovskiy, O. Korablev, Y. K. Kalinnikov, A. Fedorova, A. V. Stepanov, A. Y. Titov, et al., "Near-infrared echelle-AOTF spectrometer ACS-NIR for the ExoMars Trace Gas Orbiter," *Proc. SPIE* **9608**, 960809 (2015).
- [23] E. Dekemper, N. Loodts, B. Van Opstal, J. Maes, F. Vanhellefont, N. Matashvili, et al., "Tunable acousto-optic spectral imager for atmospheric composition measurements in the visible spectral domain," *Appl. Opt.* **51**, 6259-6267 (2012).
- [24] E. Dekemper, D. Fussen, B. Van Opstal, J. Vanhamel, D. Pieroux, F. Vanhellefont, et al., "ALTIUS: a spaceborne AOTF-based UV-VIS-NIR hyperspectral imager for atmospheric remote sensing," *Proc. SPIE* **9241**, 92410L (2014).
- [25] H. Zhang, X. L. Wang, J. I. Soos, and J. A. Crisp, "Design of a miniature solid state NIR spectrometer," *Proc. SPIE* **2475**, 376 (1995).
- [26] D. A. Glenar, D. L. Blaney, and J. J. Hillman, "AIMS: Acousto-optic imaging spectrometer for spectral mapping of solid surfaces," *Acta Astronautica* **52**, 389-396 (2003).
- [27] R. Tawalbeh, D. Voelz, D. Glenar, X. Xiao, N. Chanover, R. Hull, and D. Kuehn, "Infrared acousto-optic tunable filter point spectrometer for detection of organics on mineral surfaces," *Opt. Eng.* **52**, 3604 (2013).
- [28] S. N. Mantsevich, O. I. Korablev, Y. K. Kalinnikov, A. Y. Ivanov, and A. V. Kiselev, "Wide-aperture TeO<sub>2</sub> AOTF at low temperatures: Operation and survival," *Ultrasonics* **59**, 50-58 (2015).
- [29] V. Leroi, J.-P. Bibring, and M. Berthe, "Micromega/IR: Design and status of a near-infrared spectral microscope for in situ analysis of Mars samples," *Planet. Space Sci.* **57**, 1068-1075 (2009).
- [30] C. Pilorget, "Microscopie hyperspectrale dans le proche IR pour l'analyse in situ d'échantillons : l'instrument MicroMega à bord des missions Phobos Grunt, Hayabusa-2 et ExoMars," These de doctorat (Université Paris-Sud XI, Institut d'Astrophysique Spatiale (IAS) Bat 121, 91405 Orsay Cedex, France, 2012), 254p.
- [31] J.-P. Bibring, C. Pilorget, C. Evesque, and V. Hamm, "MicrOmega: A Hyperspectral NIR Microscope on Board Hayabusa2," *LPI Contributions* **1667**, 6399 (2012).
- [32] C. Pilorget, J.-P. Bibring, and MicrOmega Team, "The MicrOmega Instrument Onboard ExoMars and Future Missions: An IR Hyperspectral Microscope to Analyze Samples at the Grain Scale and Characterize Early Mars Processes," *LPI Contributions* **1680**, 7006 (2012).
- [33] Z. P. He, B. Y. Wang, G. Lv, C. L. Li, L. Y. Yuan, R. Xu, K. Chen, and J. Y. Wang, "Visible and Near-infrared Imaging Spectrometer (VNIS) for Chang'E-3," *Proc. SPIE* **9263**, 92630D (2014).
- [34] Z. P. He, R. Xu, C. L. Li, G. Lv, L. Y. Yuan, B. Y. Wang, R. Shu, and J. Y. Wang, "Visible and Near-Infrared Imaging Spectrometer (VNIS) For In Situ Lunar Surface Measurements," *Proc. SPIE* **9639**, 96391S (2015).
- [35] O. Korablev, A. Ivanov, A. Fedorova, Y. K. Kalinnikov, A. Shapkin, S. Mantsevich, et al., "Development of a mast or robotic arm-mounted infrared AOTF spectrometer for surface Moon and Mars probes," *Proc. SPIE* **9608**, 960807 (2015).
- [36] T. Fouchet, F. Montmessin, O. Forni, S. Maurice, R. C. Wiens, J. R. Johnson, et al., "The Infrared Investigation on the SuperCam Instrument for the Mars2020 Rover," *LPI contributions* **1832**, 1736 (2015).
- [37] V. I. Pustovoyt, and V. E. Pozhar, "Acousto-optic spectrometers for Earth remote sensing," *Proc. SPIE* **3750**, 243 (1999).
- [38] O. Korablev, J. L. Bertaux, E. Dimarellis, A. Grigoriev, Y. Kalinnikov, A. Stepanov, and S. Guibert, "An AOTF-based spectrometer for Mars atmosphere sounding," *Proc. SPIE* **4818**, 261-271 (2002).
- [39] V. B. Voloshinov, V. Y. Molchanov, and T. M. Babkina, "Acousto-optic filter of nonpolarized electromagnetic radiation," *J. Technical Phys.* **45**, 1186-1191 (2000).